
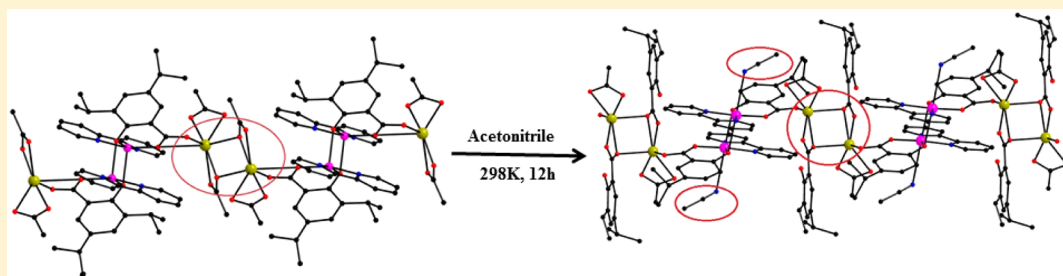


Isolation of a Metastable Intermediate in a Heterometallic Cu^{II}–Hg^{II} 1D Polymeric Chain: Synthesis, Crystal Structure, and Photophysical Properties

Shaikh M. Mobin,* Veenu Mishra, and Archana Chaudhary

Discipline of Chemistry, School of Basic Sciences, Indian Institute of Technology Indore, Khandwa Road, Indore 452017, India

 Supporting Information



ABSTRACT: A metastable heterometallic intermediate, $[\text{Cu}_2(\text{bpy})_2(\text{DIPSA})_2\text{Hg}_2(\text{OAc})_4(\text{DIPSA})_2]_n$ (**1**, where $\text{OAc} = \text{CH}_3\text{COO}^-$, $\text{bpy} = \text{bipyridine}$, and $\text{DIPSA} = \text{diisopropylsalicylic acid}$), has been isolated and characterized during the synthesis of 1D polymer $[\text{Cu}_2(\text{bpy})_2(\text{DIPSA})_2(\text{CH}_3\text{CN})_2\text{Hg}_2(\text{OAc})_2(\text{DIPSA})_4]_n$ (**2**) at ambient temperature in acetonitrile. Moreover, recrystallization of **2** in methanol results in monomeric $[\text{Cu}(\text{DIPSA})(\text{bpy})(\text{CH}_3\text{OH})] \cdot \text{CH}_3\text{OH}$ (**3**). Complexes **1–3** have been characterized by elemental analysis, Fourier transform infrared, and UV–vis spectroscopy as well as by their single-crystal X-ray structures. The photophysical study suggests the quenching of fluorescence of DIPSA upon complexation.

INTRODUCTION

Heterometallic transition-metal coordination polymers represent an actively pursued topic in modern coordination chemistry,¹ reflecting the fact that heterometallic complexes have significant applications in catalysis,² electrical conductivity,³ sensing,⁴ and magnetism.⁵ Heterometallic catalysts, where multiple metal centers are present in close proximity to each other, exhibit better reactivity than equivalent mixtures of monometallic complexes.^{2c,6} Moreover, heterometallic coordination polymers are also appealing from the crystallographic point of view owing to their diverse geometrical arrangements.⁷

Out of several approaches for the construction of heterometallic complexes, one is based on the idea that different metals show different affinities for a particular donor atom and, thus, the addition of a ligand possessing different donor atoms with a mixture of metals leads to self-assembled or well-ordered heterometallic systems.⁸ In the 5d transition metals, Hg is known to be a good candidate for generating heterometallic complexes with various other metal ions.⁹ It forms dinuclear, trinuclear, tetranuclear, and polynuclear complexes with different metals; however, it exhibits a better compatibility with Cu^{II} metal.¹⁰ These aspects extend the impetus to introduce newer routes for the construction of heterometallic complexes. Moreover, the isolation and structural characterization of a metastable intermediate is a formidable challenge. In the literature, there are only a few reports dealing with structurally characterized discrete metastable intermediates.¹¹

Herein, we report the isolation as well as structural characterization of a kinetically controlled metastable heterometallic 1D polymeric intermediate, $[\text{Cu}_2(\text{bpy})_2(\text{DIPSA})_2\text{Hg}_2(\text{OAc})_4(\text{DIPSA})_2]_n$ (**1**, where $\text{OAc} = \text{CH}_3\text{COO}^-$, $\text{bpy} = \text{bipyridine}$, and $\text{DIPSA} = \text{diisopropylsalicylic acid}$), along with the thermodynamically driven Cu^{II}–Hg^{II} 1D polymeric chain $[\text{Cu}_2(\text{bpy})_2(\text{DIPSA})_2(\text{CH}_3\text{CN})_2\text{Hg}_2(\text{OAc})_2(\text{DIPSA})_4]_n$ (**2**) and a monomeric Cu^{II} complex, $[\text{Cu}(\text{DIPSA})(\text{bpy})(\text{CH}_3\text{OH})] \cdot \text{CH}_3\text{OH}$ (**3**), obtained during recrystallization of **2** in methanol (MeOH). To the best of our knowledge, this is the first report dealing with the structural characterization of a heterometallic 1D polymeric chain intermediate.

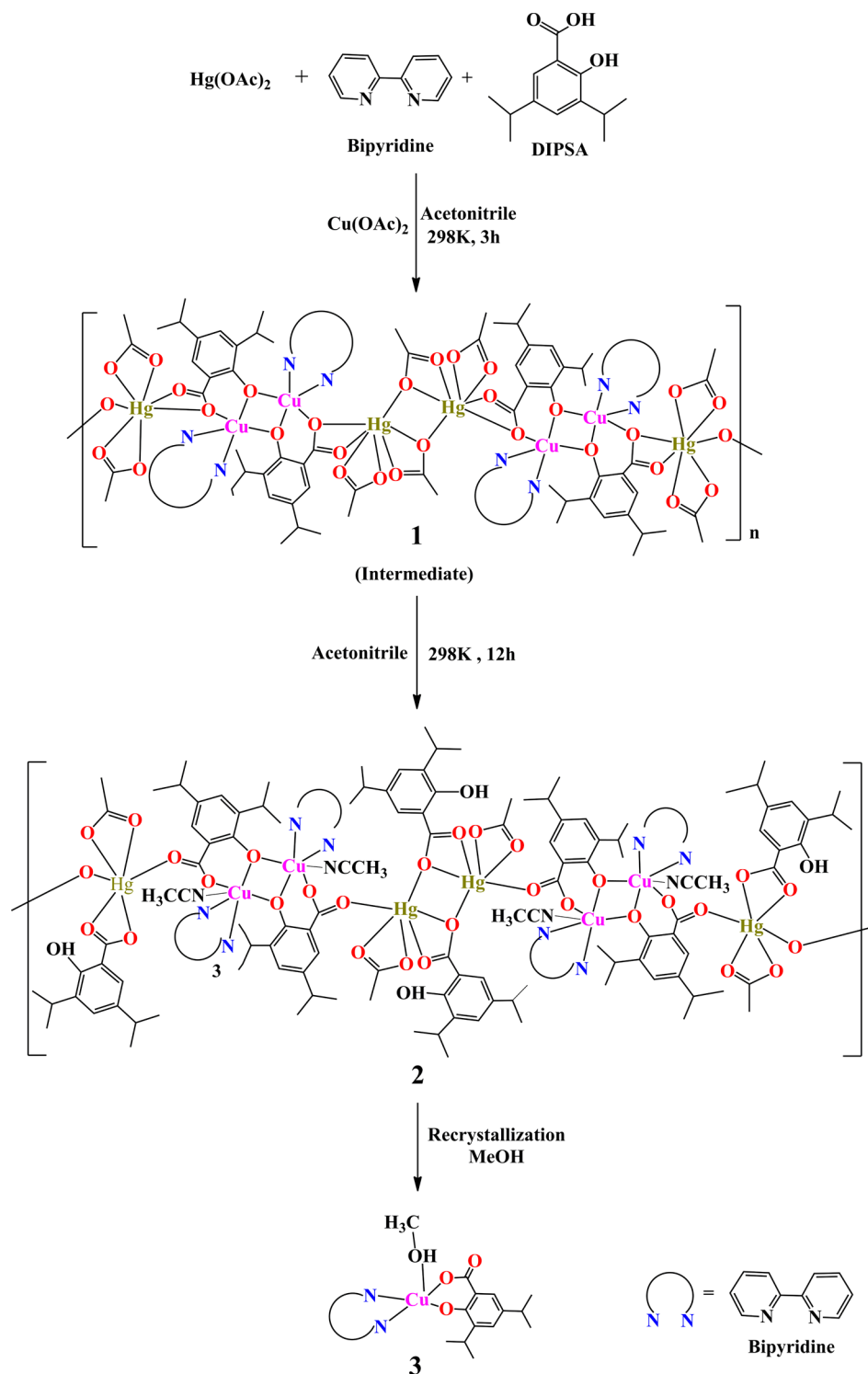
RESULTS AND DISCUSSION

Coordination polymer **2** was synthesized via the reaction of $\text{Hg}(\text{OAc})_2$, $\text{Cu}(\text{OAc})_2 \cdot \text{H}_2\text{O}$, bpy , and DIPSA in acetonitrile (ACN) at 298 K. The initial reaction mixture was dark green after 3 h and turned to light green within 12 h. A fraction of the dark-green reaction mixture was therefore extracted after 3 h, and a single spot on the thin-layer chromatography (TLC) plate ensured the presence of only one component. Its subsequent crystallization established the isolation of the kinetically driven intermediate **1**. The further extension of the same reaction up to 12 h led to the isolation of the thermodynamically stable form **2** (Scheme 1). Moreover,

Received: August 16, 2014

Published: January 23, 2015

Scheme 1. Outline of the Reactions Leading to the Formation of 1–3



recrystallization of **2** in MeOH serendipitously resulted in the new Cu^{II} monomer **3** via the breaking of the Cu^{II}–Hg^{II}-based polymer **2**. The coordinated ACN molecule from the symmetric Cu^{II} dimeric $[\text{Cu}(\text{bpy})(\text{DIPSA})(\text{CH}_3\text{CN})]_2$ unit in **2** was replaced by a MeOH molecule in **3** probably because of the formation of a stronger Cu–O bond (Scheme 1).

1–3 have been characterized by elemental analysis, Fourier transform infrared, UV–vis spectroscopy, and single-crystal X-

ray studies. The photophysical properties of all of the complexes have also been discussed.

1 crystallizes in the monoclinic space group $P2_1/c$ with a crystallographically imposed inversion center (Table 1). **1** consists of alternating dimeric units of $[\text{Cu}(\text{bpy})(\text{DIPSA})]_2$ and $[\text{Hg}(\text{OAc})_2(\text{DIPSA})]_2$. These units are connected via the same O atom of the carboxylic group of DIPSA, which generates a 1D polymeric chain (Figures 1 and S1 in the Supporting Information, SI). Each Cu atom in the dimeric $[\text{Cu}(\text{bpy})-$

Table 1. Crystallographic Details

	1	2	3
empirical formula	C ₂₇ H ₃₀ CuHgN ₂ O ₇	C ₄₀ H ₄₇ CuHgN ₃ O ₈	C ₂₅ H ₃₂ CuN ₂ O ₅
fw	758.66	961.96	504.07
temperature (K)	150(2)	150(2)	150(2)
wavelength	0.71073	0.71073	1.5418
cryst syst, space group	monoclinic, <i>P</i> 2 ₁ / <i>c</i>	triclinic, <i>P</i> $\bar{1}$	triclinic, <i>P</i> $\bar{1}$
unit cell param			
<i>a</i> (Å)	12.8050(11)	10.3212(9)	10.7914(5)
<i>b</i> (Å)	21.5075(16)	13.1358(13)	10.9401(4)
<i>c</i> (Å)	10.2905(7)	16.0182(17)	11.7748(5)
α (deg)	90	66.804(10)	90.658(3)
β (deg)	105.406(8)	79.650(8)	109.259(4)
γ (deg)	90	87.942(7)	113.692(4)
<i>V</i> (Å ³)	2732.2(4)	1962.2(3)	1184.93(9)
<i>Z</i> , <i>d</i> _{calcd} (mg/m ³)	4, 1.844	2, 1.628	2, 1.413
μ (mm ^{−1})	6.438	4.504	1.621
<i>F</i> (000)	1484	962	530
θ range (deg)	3.10–25.00	3.05–25.00	4.03–72.08
index ranges	−15 ≤ <i>h</i> ≤ 14, −25 ≤ <i>k</i> ≤ 25, −12 ≤ <i>l</i> ≤ 12	−11 ≤ <i>h</i> ≤ 12, −15 ≤ <i>k</i> ≤ 15, −13 ≤ <i>l</i> ≤ 9	−13 ≤ <i>h</i> ≤ 9, −19 ≤ <i>l</i> ≤ 18−13 ≤ <i>k</i> ≤ 13, −8 ≤ <i>l</i> ≤ 14
reflns collected/unique	20148/4803 [<i>R</i> (int) = 0.0891]	14767/6899 [<i>R</i> (int) = 0.0763]	7697/4555 [<i>R</i> (int) = 0.0127]
max and min transmn	0.7390 and 0.4882	0.3653 and 0.2939	0.7271 and 0.6087
refinement method	full-matrix least squares on <i>F</i> ²	full-matrix least squares on <i>F</i> ²	full-matrix least squares on <i>F</i> ²
data/restraints/param	4803/0/349	6899/0/488	4555/0/312
GOF, <i>F</i> ²	1.055	1.055	1.033
<i>R</i> ₁ , <i>wR</i> ₂ [<i>I</i> > 2σ(<i>I</i>)]	0.0628, 0.1537	0.0852, 0.2284	0.0344, 0.0943
<i>R</i> ₁ , <i>wR</i> ₂ (all data)	0.0831, 0.1699	0.1162, 0.2785	0.0352, 0.0952
CCDC no.	1014845	1014846	1014847

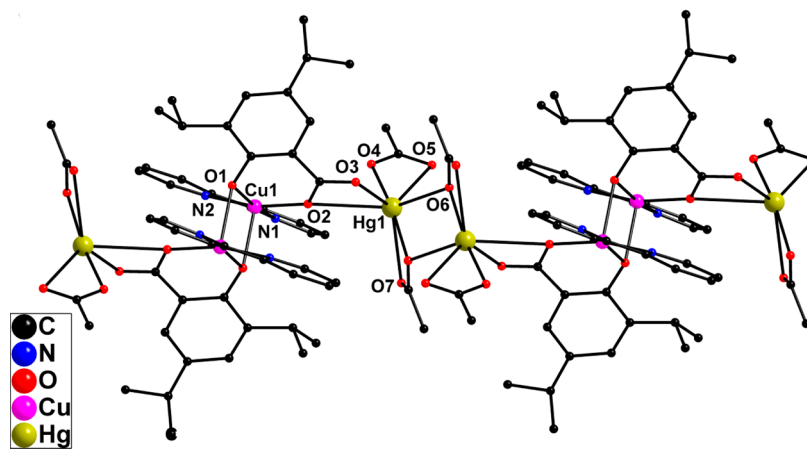


Figure 1. Perspective view of 1.

(DIPSA)]₂ unit is in an N₂O₃ environment. The Cu^{II} atom is surrounded by two N-atom donors of bpy, one carboxylic O atom, and two phenolic O atoms of DIPSA, creating a distorted square-pyramidal geometry. Phenolic O atoms bridge the neighboring Cu^{II} atoms within the dimeric [Cu(bpy)(DIPSA)]₂ unit. The average Cu–N and Cu–O distances are in the ranges of 1.995(9)–2.013(8) and 1.921(7)–2.277(6) Å, respectively (Table S1 in the SI), which are identical with the reported analogous dimers.¹² Each Hg^{II} atom in the dimeric [Hg(OAc)₂(DIPSA)]₂ unit is in an O₇ environment. The Hg^{II} atom is bonded to five O atoms from the acetate groups and two from the carboxylic groups of DIPSA, leading to a distorted pentagonal-bipyramidal geometry. Moreover, the chelated acetate groups bridge the adjacent Hg atoms in the dimeric unit [Hg(OAc)₂(DIPSA)]₂. The dimeric units [Hg-

(OAc)₂(DIPSA)]₂ consist of two different sets of Hg–O distances; the shorter and longer ranges are 2.101(9)–2.402(7) and 2.606(8)–2.870(9) Å, respectively.¹³

The packing diagram of 1 reveals the existence of intra- and intermolecular hydrogen bonding and CH– π interactions. The intramolecular hydrogen bonding involves C1–H1...O7, 2.856(1) Å, and C9–H9...O5, 2.551(1) Å, between the bpy ring and acetate group along the polymeric chain. Intermolecular hydrogen-bonding interactions are comprised of C3–H3...O3, 2.681(8) Å, between bpy and DIPSA. Moreover, the CH– π interaction, involving the H4 and H7 atoms of bpy and the π electrons of the aromatic ring of DIPSA with a distance 3.06 Å,¹⁴ forms a 2D framework along the *b* axis (Figure 2 and Figure S2 and Table S2 in the SI).

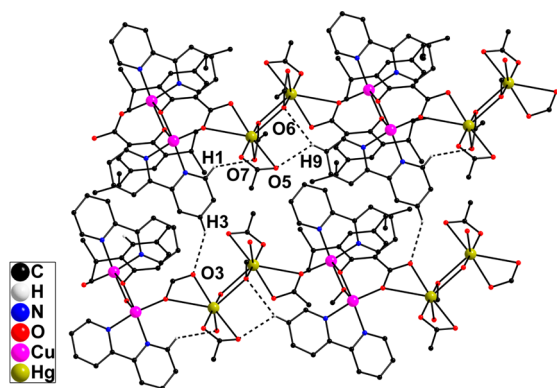


Figure 2. Packing diagram of **1** showing the intra- and intermolecular hydrogen-bonded 2D networks (H atoms are removed for clarity).

2 crystallizes in the triclinic space group $P\bar{1}$ with a crystallographically imposed inversion center (Table 1). **2** consists of two alternating dimeric units, $[\text{Cu}(\text{bpy})(\text{DIPSA})(\text{CH}_3\text{CN})_2]$ and $[\text{Hg}(\text{OAc})(\text{DIPSA})_2]$, linked via carboxylic O-atom donors of DIPSA. Unlike **1**, in **2** these Cu and Hg units are connected by different O atoms of the same carboxylic group of DIPSA. In contrast to **1**, in **2** each Cu^{II} ion in dimeric $[\text{Cu}(\text{bpy})(\text{DIPSA})(\text{CH}_3\text{CN})_2]$ is in an N_3O_3 environment. The basal plane consists of two N atoms of bpy and one phenolic and one carboxylic O atom of DIPSA and the axial positions are occupied by a phenolic O atom of DIPSA and a N atom of the ACN molecule, leading to a distorted octahedral geometry (Figures 3 and S3 in the SI). The adjacent Cu atoms

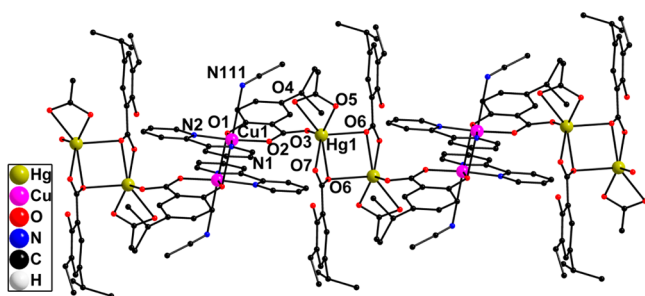


Figure 3. Perspective view of **2**.

in the dimeric unit are connected via phenolic O atoms of different DIPSA molecules. The average Cu–N and Cu–O distances are between 2.005(10) and 2.007(12) and 1.888(9) and 1.938(9) Å, respectively (Table S1 in the SI). In the dimeric $[\text{Hg}(\text{OAc})(\text{DIPSA})_2]$ unit, a Hg^{II} atom is bonded to two O atoms of the bidentate acetate group and four carboxylic groups of DIPSA, leading to a distorted octahedral arrangement. The two O atoms of different DIPSA molecules are connected to the neighboring Cu atoms, and another O atom of DIPSA is working as a bridge between Cu- and Hg-derived dimeric units. The remaining one O atom of DIPSA is coordinated to one Hg^{II} atom only. The average Hg–O distances are in the range of 2.154(1)–2.589(1) Å.

The packing diagram of **2** reveals the presence of intra- and intermolecular hydrogen-bonding interactions. Intramolecular interactions involve C9–H9...O5, 2.527(1) Å, and C9–H9...O6, 2.684(1) Å, between bpy and the acetate group. Further, it shows the presence of stronger O8–H108...O7, 1.844(1) Å, nonbonding interaction between an H atom of the hydroxyl

group of DIPSA and an O atom of the carboxylate group of the same DIPSA group. The coordinated ACN molecule is trapped between the two adjacent layers of the 1D polymeric chain and develops the hydrogen-bonding interaction via C4–H4...N333 with a distance of 2.459(6) Å, which indeed leads to the formation of a 2D network (Figure 4 and Figures S4 and S5 and Table S2 in the SI).

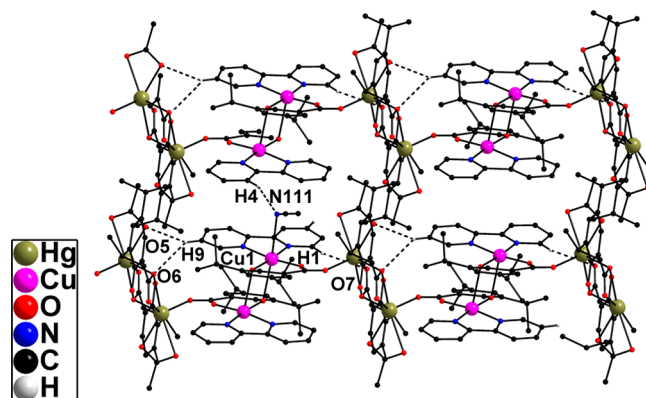


Figure 4. Packing diagram of **2**, where ACN molecules are trapped between two 1D chains, forming a 2D polymeric framework (H atoms are removed for clarity).

In **1** and **2**, all of the ligands are in the trans orientation. The transformation of **1** to **2** involves the replacement of two of the acetate groups in the Hg^{II} dimer by bulky DIPSA molecules, followed by coordination of the ACN solvent to the Cu^{II} center in the dimeric unit. The symmetric Cu_2O_2 and Hg_2O_2 rings in **1** and **2** are planar. In **1** and **2**, the Cu_2O_2 ring is deviated from Hg_2O_2 by angles of 71.85° and 72.43°, respectively. The estimated dihedral angles between the bpy and DIPSA rings in the Cu^{II} dimeric units of **1** and **2** are 64.10° and 17.89°, respectively.

A plausible mechanism for the transformation of **1** to **2** is depicted in Scheme 2. The common feature in **1** and **2** is the presence of the stable Cu^{II} dimeric unit $[\text{Cu}(\text{bpy})(\text{DIPSA})_2]$. However, the Hg^{II} -derived dimeric unit $[\text{Hg}(\text{OAc})_2(\text{DIPSA})_2]$ undergoes the major transformation in the form of replacement of the bridging acetate groups¹⁵ by DIPSA as acetic acid.¹⁶ Moreover, the strong intramolecular hydrogen bonding between H atom of the phenolic group O8 and the carboxylic O7 of DIPSA might have extended the necessary driving force toward stabilization of **2**.¹⁷

3 crystallizes in the triclinic space group $P\bar{1}$ (Table 1). The Cu^{II} ion in the monomer unit $[\text{Cu}(\text{bpy})(\text{DIPSA})(\text{CH}_3\text{OH})]$ ·CH₃OH is in an N_2O_3 environment. The basal plane consists of two N atoms of bpy and one phenolic and one carboxylic O atom of DIPSA, while the apical position is occupied by the O atom of the solvent molecule (MeOH). This in effect leads to a distorted square-pyramidal geometry (Figure 5). The Cu–O and Cu–N bond distances are Cu1–O1 1.897(1) Å, Cu1–O3 1.877(1) Å, and Cu1–O111 2.544(4) and ≈2.00 Å, respectively (Table S1 in the SI).

The packing diagram of monomeric **3** reveals intermolecular hydrogen-bonding and π – π interactions. Intermolecular hydrogen-bonding interaction C8–H8...O2, 2.523(1) Å, between bpy and DIPSA leads to the formation of a 1D layer, which has been further extended via C4–H4...O111, 2.466(2) Å, and C7–H7...O111, 2.691(2) Å, interactions between bpy and coordinated MeOH. The π – π interaction between two bpy

Scheme 2. Probable Reaction Pathway Toward the Transformation of 1 to 2

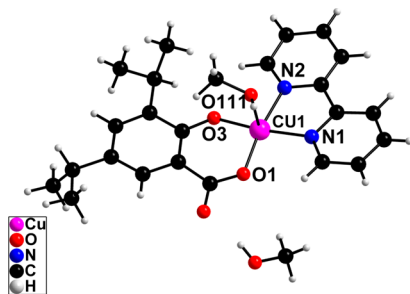
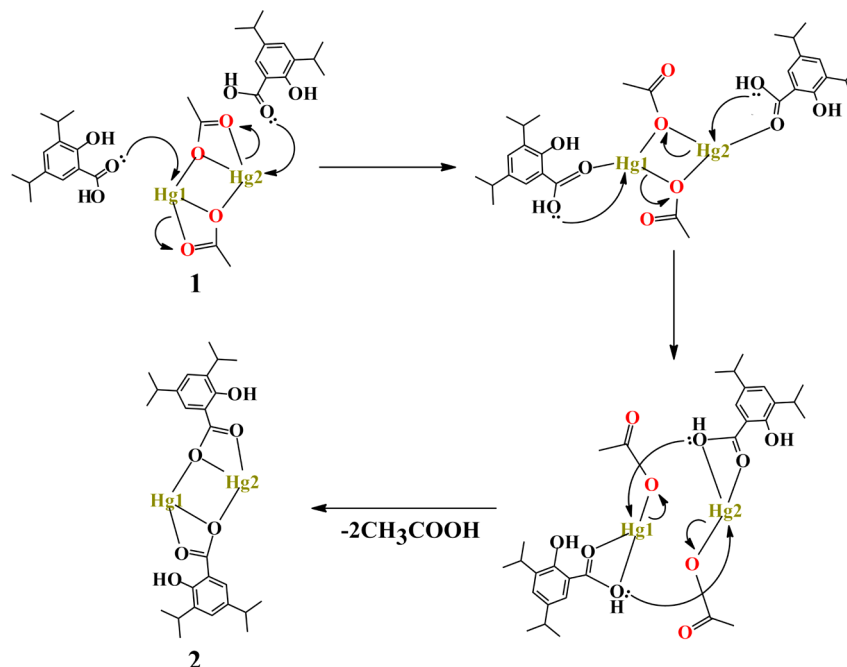


Figure 5. Perspective view of 3.

rings of two monomeric units with a distance of 3.360 Å results in a 2D network (Figure 6 and Figures S6 and S7 and Table S2 in the SI).

Electronic absorption and emission spectra of 1–3 and DIPSA have been recorded in MeOH. DIPSA shows a peak at 314 nm and a shoulder at 240 nm due to $\pi-\pi^*$ and $n-\pi^*$ transitions, respectively.¹⁸ Upon complexation with metal, the $\pi-\pi^*$ band is found to be blue-shifted by 8–10 nm and the

$n-\pi^*$ band disappears. The blue shift of the $\pi-\pi^*$ transition might have taken place because of the destruction of hydrogen bonding between the phenolic and carboxyl functions of DIPSA during the complexation process.¹⁹

The highly fluorescent DIPSA ligand exhibits an emission band at 412 nm upon excitation at 314 nm with a calculated quantum yield of 0.29. However, the emission intensity of the complexes is quenched appreciably with the red-shifted band at 424 nm. The estimated quantum yields of 1–3 of 0.11, 0.13, and 0.09, respectively, are quite less compared to the pure ligand. The quenching in fluorescence of the free ligand upon complexation must be attributed to the presence of well-known fluorescent quencher Hg^{II} and Cu^{II} metal ions (Figures 7 and 8).²⁰

CONCLUSION

This paper demonstrates the isolation and structural characterization of the first example of the kinetically driven heterometallic polymeric intermediate, 1 along with a thermodynamically controlled 1D polymeric chain, 2. The transformation of 1 to 2 essentially takes place via the partial

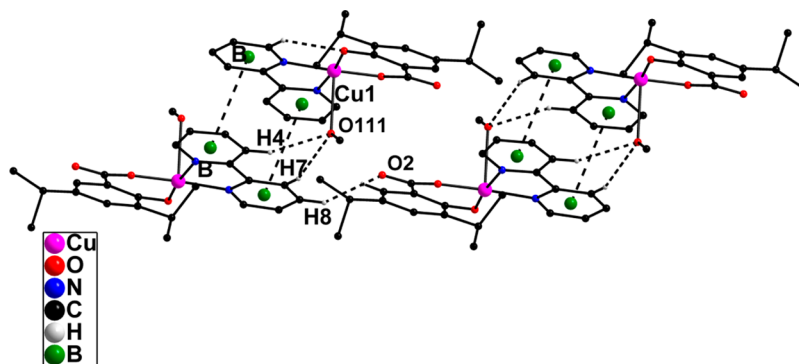


Figure 6. Packing diagram of 3 showing a 2D polymeric chain formed via intermolecular hydrogen-bonding and $\pi-\pi$ interaction (H atoms are removed for clarity).

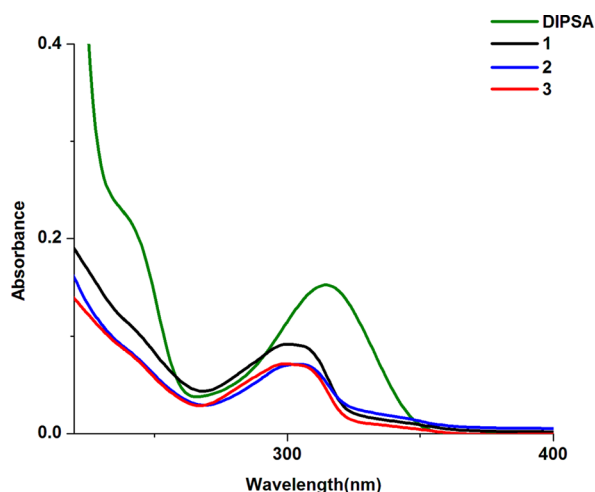


Figure 7. Absorption spectra of DIPSA and 1–3.

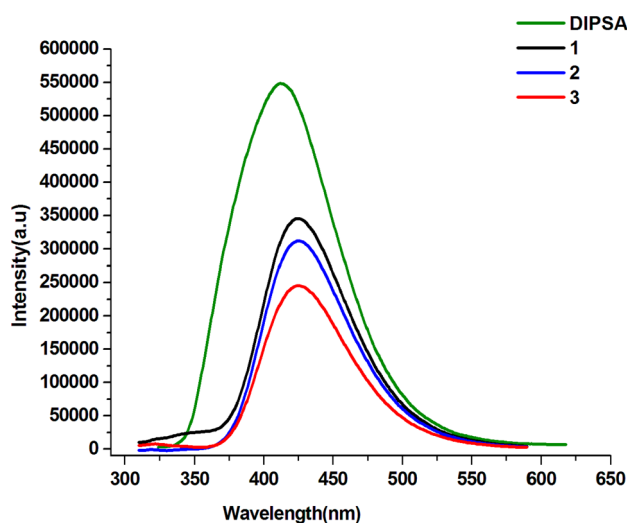


Figure 8. Emission spectra of DIPSA and 1–3 showing fluorescence quenching.

replacement of the OAc group by the DIPSA ligand around the Hg centers, keeping the Cu centers unaltered. Strong intramolecular hydrogen bonding between the H atom of the phenolic group and the carboxylic O atom of DIPSA plays a vital role in stabilizing **2**. To our surprise, **2** upon recrystallization from MeOH changes to the Cu^{II}-based monomeric complex **3** via the ACN/MeOH exchange process.

EXPERIMENTAL DETAILS

Materials. The commercially available starting materials Cu(CH₃COO)₂·H₂O, Hg(CH₃COO)₂, bipyridine (bpy), and diisopropylsalicylic acid (DIPSA) and reagent-grade solvents (MeOH and ACN) were used as received.

Instruments. IR spectra (4000–400 cm^{−1}) were recorded with a Bio-Rad FTS 3000MX instrument on KBr pellets. Elemental analyses were carried out with a Flash 2000 elemental analyzer. UV spectra were recorded on a Cary-100 Bio UV–vis spectrophotometer. Fluorescence spectra of all of the compounds were recorded on a Horiba Jobin-Yvon Fluoromax 4P spectrophotometer. Single-crystal X-ray structural studies were performed on an Agilent Technology Supernova CCD diffractometer equipped with a low-temperature attachment.

X-ray Crystallography. Data were collected at 150(2) K using graphite-monochromated Mo Kα ($\lambda_{\alpha} = 0.71073$ Å) and Cu Kα ($\lambda_{\alpha} =$

1.54814 Å). The strategy for data collection was evaluated using the *CrysAlisPro* CCD software. The data were collected by the standard ϕ – ω scan techniques and scaled and reduced using *CrysAlisPro RED* software. The structures were solved by direct methods using *SHELXS-97* and refined by full-matrix least squares with *SHELXL-97* on F^2 .²¹ The positions of all of the atoms were obtained by direct methods. All non-H atoms were refined anisotropically. The remaining H atoms were placed in geometrically constrained positions and refined with isotropic temperature factors, generally 1.2 U_{eq} of their parent atoms. All of the hydrogen-bonding interactions, mean-plane analyses, and molecular drawings were obtained using the *Diamond* program (version 3.1d). The crystal and refinement data are summarized in Table 1, and selected bond distances and angles are shown in Table S1 in the SI.

Synthesis of 2. A solution of Hg(CH₃COO)₂ (0.318 g, 1 mmol) and bpy (0.156 g, 1 mmol), and DIPSA (0.222 g, 1 mmol) in ACN was stirred for 15 min, and then Cu(CH₃COO)₂·H₂O (0.0497 g, 0.25 mmol) was added. The entire contents were stirred magnetically for 3 h at 298 K. The color of the reaction mixture was dark green after 3 h, so a fraction of the reaction mixture was extracted after 3 h. In this mixture, we observed a single-spot TLC, ensuring the presence of only one component in the system, so it was left for crystallization and was characterized as intermediate **1**. When the reaction time was exceeded, the color of the solution turned to light green after 12 h. Upon extension of the reaction time to more than 12 h, no remarkable changes were observed. The progress of the reaction was monitored by TLC. The solution was then passed through filter paper (Whatman filter paper, 70 mm) in order to remove any unreacted materials. The filtrate was allowed to stand at 298 K for crystallization. Upon slow evaporation of the solvent, light-green single crystals of **2** were obtained after 2 weeks.

Anal. Calcd for **1** [C₂₇H₃₀CuHgN₂O₇ ($M_w = 758.66$)]: C, 42.79; H, 3.99; N, 3.68. Found: C, 42.84; H, 3.97; N, 2.97.

Anal. Calcd for **2** [C₄₀H₄₇CuHgN₃O₈ ($M_w = 961.96$)]: C, 49.99; H, 4.82; N, 4.37. Found: C, 49.55; H, 4.79; N, 4.30. IR (KBr, cm^{−1}): ν 3419 (br), 1570 (s), 1442 (s), 1245 (w), 1168 (w), 887 (s), 768 (s).

Synthesis of 3. When complex **2** was kept for recrystallization in MeOH, compound **3** was obtained after 8 days. Anal. Calcd for C₂₅H₃₂CuN₂O₅ ($M_w = 504.07$): C, 59.57; H, 6.40; N, 5.56. Found: C, 59.55; H, 6.79; N, 5.30. IR (KBr, cm^{−1}): ν 3422 (br), 1605 (s), 1567 (s), 1443 (s), 1309 (w), 1248 (w), 1167 (w), 1027 (m), 768 (s).

ASSOCIATED CONTENT

Supporting Information

Bond angles and distances and hydrogen-bonding details (Tables S1 and S2) and packing diagrams (Figures S1–S7). This material is available free of charge via the Internet at <http://pubs.acs.org>.

AUTHOR INFORMATION

Corresponding Author

*E-mail: xray@iiti.ac.in.

Author Contributions

The manuscript was written through contributions of all authors. All authors have given approval to the final version of the manuscript.

Notes

The authors declare no competing financial interest.

ACKNOWLEDGMENTS

We are grateful to the single-crystal X-ray diffraction facility equipped at the Sophisticated Instrumentation Centre, IIT Indore. S.M.M. thanks the CSIR New Delhi for a research grant.

REFERENCES

- (1) (a) Ciurtin, D. M.; Smith, M. D.; zur Loye, H.-C. *Dalton Trans.* **2003**, 1245–1250. (b) Song, J.-L.; Mao, J.-G.; Zeng, H.-Y.; Dong, Z.-C. *Eur. J. Inorg. Chem.* **2004**, 538–543. (c) Burrows, A. D.; Cassar, K.; Mahon, M. F.; Warren, J. E. *Dalton Trans.* **2007**, 2499–2509. (d) Ellsworth, J. M.; zur Loye, H.-C. *Dalton Trans.* **2008**, 5823–5835. (e) Das, L. K.; Kadam, R. M.; Bauza, A.; Frontera, A.; Ghosh, A. *Inorg. Chem.* **2012**, 51, 12407–12418. (f) Shaikh, M. M.; Mishra, V.; Ram, P.; Birla, A.; Mathur, P. *Dalton Trans.* **2013**, 42, 10687–10689. (g) Ma, Y.-Z.; Zhang, L.-M.; Peng, G.; Zhao, C.-J.; Dong, R.-T.; Yang, C.-F.; Deng, H. *CrysEngComm* **2014**, 16, 667–683. (h) Shaikh, M. M.; Mishra, V.; Chaudhary, A.; Rai, D. K.; Golov, A. A.; Mathur, P. *Cryst. Growth Des.* **2014**, 14, 4124–4137.
- (2) (a) Nesterov, D. S.; Chygorin, E. N.; Kokozay, V. N.; Bon, V. V.; Boča, R.; Kozlov, Y. N.; Shul'pina, L. S.; Jezierska, J.; Ozarowski, A.; Pombeiro, A. J. L.; Shul'pin, G. B. *Inorg. Chem.* **2012**, 51, 9110–9122. (b) Wimberg, J.; Meyer, S.; Dechert, S.; Meyer, F. *Organometallics* **2012**, 31, 5025–5033. (c) Mata, J. A.; Ekkehardt Hahn, F.; Peris, E. *Chem. Sci.* **2014**, 5, 1723–1732.
- (3) Doménech, A.; Koshevoy, I. O.; Montoya, N.; Pakkanen, T. A. *Anal. Bioanal. Chem.* **2010**, 397, 2013–2022.
- (4) (a) Saha, D.; Das, S.; Maity, D.; Dutta, S.; Baitalik, S. *Inorg. Chem.* **2011**, 50, 46–61. (b) Chakrabarty, P. P.; Sahaa, S.; Sen, K.; Jana, A. D.; Dey, D.; Schollmeyer, D.; Granda, S. G. *RSC Adv.* **2014**, 4, 40794–40802.
- (5) Li, Y.-Y.; Yan, B.; Li, Q.-P. *Dalton Trans.* **2013**, 42, 1678–1686.
- (6) Park, J.; Hong, S. *Chem. Soc. Rev.* **2012**, 41, 6931–6943.
- (7) (a) Leznoff, D. B.; Draper, N. D.; Batchelor, R. J. *Polyhedron* **2003**, 22, 1735–1743. (b) Ahern, J. C.; Roberts, R. J.; Follansbee, P.; McLaughlin, J.; Leznoff, D. B.; Patterson, H. H. *Inorg. Chem.* **2014**, 53, 7571–7579.
- (8) (a) Novitchi, G.; Shova, S.; Caneschi, A.; Costes, J.-P.; Gdaniec, M.; Stanica, N. *Dalton Trans.* **2004**, 1194–1200. (b) Biswas, S.; Naiya, S.; Gomez-Garcia, C. J.; Ghosh, A. *Dalton Trans.* **2012**, 41, 462–473. (c) Tereniak, S. J.; Carlson, R. K.; Clouston, L. J.; Young, V. G., Jr.; Bill, E.; Maurice, R.; Chen, Y.-S.; Kim, H. J.; Gagliardi, L.; Lu, C. C. *J. Am. Chem. Soc.* **2014**, 136, 1842–1855.
- (9) (a) Bullock, S.; Gillie, L. J.; Harding, L. P.; Rice, C. R.; Riis-Johannessen, T.; Whitehead, M. *Chem. Commun.* **2009**, 4856–4858. (b) Chygorin, E. N.; Nesterova, O. V.; Rusanova, J. A.; Kokozay, V. N.; Bon, V. V.; Boc, R.; Ozarowski, A. *Inorg. Chem.* **2012**, 51, 386–396. (c) Karmakar, D.; Fleck, M.; Saha, R.; Layek, M.; Kumar, S.; Bandyopadhyay, D. *Polyhedron* **2013**, 49, 93–99.
- (10) (a) Dong, Y. B.; Smith, M. D.; zur Loye, H.-C. *Angew. Chem., Int. Ed.* **2000**, 39, 4271–4273. (b) Patel, U.; Singh, H. B.; Wolmershauser, G. *Angew. Chem., Int. Ed.* **2005**, 44, 1715–1717. (c) Nayak, M.; Sarkar, S.; Hazra, S.; Sparkes, H. A.; Howard, J. A. K.; Mohanta, S. *CrysEngComm* **2011**, 13, 124–132. (d) Biswas, S.; Saha, R.; Ghosh, A. *Organometallics* **2012**, 31, 3844–3850.
- (11) (a) Storre, J.; Schnitter, C.; Roesky, H. W.; Schmidt, H.-G.; Noltemeyer, M.; Fleischer, R.; Stalke, D. *J. Am. Chem. Soc.* **1997**, 119, 7505–7513. (b) Patmore, N. J.; Mahon, M. F.; Steed, J. W.; Weller, A. S. *J. Chem. Soc., Dalton Trans.* **2001**, 277–283. (c) Coggins, M. K.; Sun, X.; Kwak, Y.; Solomon, E. I.; Akimova, E. R.; Kovacs, J. A. *J. Am. Chem. Soc.* **2013**, 135, 5631–5640.
- (12) (a) Craven, E.; Zhang, C.; Janiak, C.; Rheinwald, G.; Lang, H. Z. *Anorg. Allg. Chem.* **2003**, 629, 2282–2290. (b) Sun, J.; Xu, H. *Molecules* **2010**, 15, 8349–8359.
- (13) Tikhonova, I. A.; Tugashov, K. I.; Dolgushin, F. M.; Korlyukov, A. A.; Petrovskii, P. V.; Klemenkova, Z. S.; Shur, V. B. *J. Organomet. Chem.* **2009**, 694, 2604–2610.
- (14) (a) Carballo, R.; Covelo, B.; Ezequiel, M.; Vazquez-Lopez, E.; Garcia-Martinez, A.-C.; Niclos, J. Z. *Anorg. Allg. Chem.* **2005**, 631, 785–792. (b) Tsuzuki, S. *Annu. Rep. Prog. Chem., Sect. C: Phys. Chem.* **2012**, 108, 69–95.
- (15) (a) Mukherjee, A.; Saha, M. K.; Rudra, I.; Ramasesha, S.; Nethaji, M.; Chakravarty, A. R. *Inorg. Chim. Acta* **2004**, 357, 1077–1082. (b) Mukherjee, A.; Saha, M. K.; Nethaji, M.; Chakravarty, A. R. *Polyhedron* **2004**, 23, 2177–2182. (c) Chandrasekhar, V.; Senapati, T.; Dey, A.; Sanudo, E. C. *Inorg. Chem.* **2011**, 50, 1420–1428.
- (16) Casarin, M.; Cingolani, A.; Nicola, C. D.; Falcomer, D.; Monari, M.; Pandolfo, L.; Pettinari, C. *Cryst. Growth Des.* **2007**, 7, 676–685.
- (17) Ng, V. W. L.; Taylor, M. K.; White, J. M.; Young, C. G. *Inorg. Chem.* **2010**, 49, 9460–9469.
- (18) Greenway, L. J.; Norris, F. T. *Inorg. Chim. Acta* **1988**, 145, 279–284.
- (19) Brumas, V.; Miche, H.; Fiallo, M. J. *Inorg. Biochem.* **2007**, 101, 565–577.
- (20) (a) Akkaya, E. U.; Huston, M. E.; Czarnik, A. W. *J. Am. Chem. Soc.* **1990**, 112, 3590–3593. (b) Kumar, I.; Ghosh, R. P. *Inorg. Chem.* **2011**, 50, 4229–4231. (c) Quang, D. T.; Hop, N. V.; Luyen, N. D.; Thu, H. P.; Oanh, D. Y.; Hien, N. K.; Hieu, N. V.; Lee, M. H.; Kime, J. S. *Luminescence* **2013**, 28, 222–225.
- (21) Sheldrick, G. M. *Acta Crystallogr., Sect. A* **2008**, A64, 112–122. *Program for Crystal Structure Solution and Refinement*; University of Göttingen: Göttingen, Germany, 1997.